Effects of annealing atmosphere on the structural and optical properties of ZnMgO thin films grown by RF magnetron sputtering

F. ZHAO[a], J. H. TAO[a], Y. X. GUO[a], C. H. MA[a], F. W. SHI[a,b,*], J. C. JIANG[a,b,*], Z. G HU[a], J. H. CHU[a,b c]
[a]*Key Laboratory of Polar Materials and Devices, Ministry of Education, Department of Electronic Engineering, East China Normal University, Shanghai 200241, China*
[b]*Shanghai Center for Photovoltaics, Shanghai 201201, China*
[c]*Shanghai Institute of Technical Physics, Chinese Academy of Sciences, Shanghai 200083, China*

ZnMgO thin films were deposited on quartz substrates by radio frequency (RF) magnetron sputtering. For comparison, two series of identical films were then annealed in air and vacuum atmosphere at temperature in a range of 340–500 ℃, respectively. The structural and optical properties of the ZnMgO films were systematically investigated by X-ray diffraction (XRD), scanning electronic microscopy (SEM), spectrophotometer and photoluminescence (PL) spectra. Experimental results indicate that compared with vacuum annealing, air annealing can promote the formation of ZnMgO nanocrystals. At the same annealing temperature, the samples annealed in air have a more nanocrystalline number, larger size, better uniformity and higher PL peak intensity than the vacuum annealed samples. However, the optical band gap of the film annealed in air is narrower than that of the sample annealed in vacuum. Furthermore, the samples annealed in air atmosphere at 420 ℃ have the largest number of nanocrystals and the largest size (19.14 nm). These results demonstrate that high quality ZnMgO nanocrystals can be precipitated by air annealing.

(Received June 5, 2018; accepted April 8, 2019)

Keywords: ZnMgO thin films, ZnMgO nanocrystals, Magnetron sputtering, Annealing atmosphere

1. Introduction

Over the years, ZnMgO namely the alloy of ZnO, has attracted a great deal of attention, owing to its novel properties of a wide band gap, large exciton binding energy and strong bonding strength at room temperature [1-4]. In particular, it has been known that the band gap of ZnMgO can be modulated via controlling the Mg content within a certain range [5-6], which allows it to be employed for ultraviolet (UV) detectors, and solar devices [7-9]. Currently, different methods have been applied to the preparation of ZnMgO films, including chemical vapor deposition (CVD), pulsed laser deposition (PLD), sol-gel method, molecular beam epitaxy (MBE) and magnetron sputtering [10-14]. Among these techniques, the magnetron sputtering method has some excellent advantages, for example, good film-to-substrate adhesion, low cost, and low operating temperature [15-16]. However, a great deal of film flaws will be generated by applying such a high speed non-equilibrium preparation process, thence, the microstructure and optoelectronic properties will be severely affected [17-18]. It is generally affirmed that the post-annealing is a significant method for improving the crystal quality of ZnMgO thin film, because it can reduce flaws, enhance luminescent properties and regulate the optical band gaps of the films [19-20]. Up to now, there is no report on the influence of annealing atmosphere on the structural and optical characteristics of ZnMgO thin films grown by RF magnetron sputtering.

In this paper, air annealing is utilized as a replaceable method to vacuum annealing for ZnMgO nanocrystals formation. The effectiveness, as well as the merits, of the air annealing technique, with respect to vacuum annealing, in forming ZnMgO nanocrystals were investigated systematically by analyzing the structural and optical characteristics of thin films. It is shown that air annealing method can get high quality ZnMgO film.

2. Experimental detail

A ZnMgO target was prepared by a sintering mixture of 99.99 % pure MgO and ZnO powders. The ZnMgO thin films were synthesized on quartz substrates via RF magnetron sputtering. The distance is set to 6 cm between the target and the substrate. The sputtering chamber was evacuated down to 4.0×10^{-4} Pa before deposition. During the film sputtering, the ambient gases were high purity argon, and the constant flow rate of the argon and the chamber pressure was set at 40 sccm and 8×10^{-1} Pa separately. The other sputtering conditions namely substrate temperature, radio frequency sputtering power and sputtering time were fixed at 100 ℃, 150 W and 90 min, respectively. Moreover, the ZnMgO target was pre-sputtered for 15 min to remove surface contamination before film deposition. After the deposition, the samples were annealed under ambient air atmosphere at 340–500 ℃ for 20 min (temperature hold time) by a tube

furnace (sample name: A-340, A-420 and A-500, respectively). A heating velocity of 20 °C/min was utilized in all cases. For comparison with ambient air annealing, vacuum annealing at 340–500 °C for 20 min (temperature hold time) with a heating velocity of 20 °C/min in the identical tube furnace was also done for ZnMgO films (sample name: V-340, V-420 and V-500, respectively).

Crystal structures of the films were examined by X-ray diffraction (XRD, Rigku D/max 2550 V). The transmittance spectra were characterized by using a UV-VIS spectrophotometer (Cary5000). Morphologies of the films were observed via scanning electron microscopy (SEM, JEOL). Energy dispersive X-ray (EDX) spectroscopy was adopted to detect the element components, and photoluminescence (PL) spectra were measured using a He–Cd laser with an excitation wavelength of 532 nm by a Confocal Laser Raman Spectrometer (LabRAM HR 800 UV).

3. Results and discussion

3.1. Structural properties

Fig. 1a shows the XRD spectra for the ZnMgO thin film samples after vacuum and air annealing. In the spectra, all films treated at different annealing temperatures present merely a (002) diffraction peak corresponding to a c-axis oriented ZnMgO hexagonal wurtzite structure [21]. The diffraction peak intensity of the sample annealed in air is higher than those of the sample annealed in vacuum in the range of 340-500 °C, suggesting air annealing can produce more crystallization grains. In the cases of air annealing, the diffraction peak intensity increases when the annealing temperature rises from 340 °C to 420 °C, which indicates that the number of crystal grains gradually increases with the ascent of temperature. However, as the annealing temperature further rises to 500 °C, the peak intensity starts off decrease, indicating that the reduction of crystalline grains number [22]. This demonstrates the number of crystalline grains is the most at 420 °C by air annealing. Meanwhile, it can be observed that the crystallization peak intensity is also increased first and then weakened for the film annealed in vacuum at 340-500 °C. It can be seen from the Fig. 1b that the full width at half maximum (FWHM) of the samples A-340, A-420, A-500, V-340,V-420 and V-500 are 0.49°, 0.43°, 0.44°, 0.50°,0.45° and 0.46°, respectively. The FWHM of the sample annealed in air is lower than those of the sample annealed in vacuum in the range of 340-500 °C, suggesting air annealing can produce larger crystallization grains. The FWHM of the ZnMgO (002) peak is the narrowest at 420 °C by air annealing, which indicates that the growth of crystal grains can be promoted under this condition. The particle sizes of the ZnMgO films were determined by means of Debye-Scherrer formula [23]:

$$D = \frac{K\lambda}{\beta \cos\theta} \quad (1)$$

where K is a constant (<0.89), λ is the X-ray excitation wavelength (0.154 nm), θ is the Bragg angle and β is the corrected FWHM of the ZnMgO (002) XRD peak. As shown in Fig. 1c, the crystallite sizes of the sample A-340, A-420, A-500, V-340, V-420, and V-500 were 16.78 nm, 19.14 nm, 18.70 nm, 16.44 nm, 18.28 nm and 17.89 nm, respectively. This confirms that the crystalline grain of the film is nanocrystalline, which correlates to the previous analysis. The above results can be explained that the oxygen in the air atmosphere may inhibit the increase of the Mg content in the wurtzite ZnO film by air annealing, which can contribute to reduce the flaw density in wurtzite ZnO matrix and improve the crystalline quality of the film.

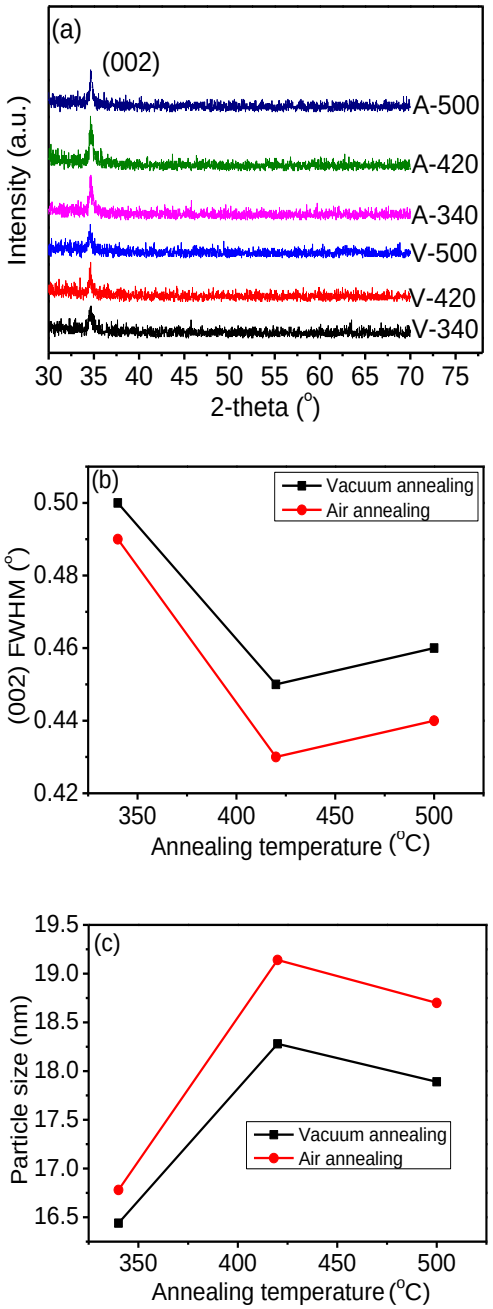

Fig. 1. (a) XRD spectra of sample A-340, A-420, A-500, V-340, V-420 and V-500, (b) FWHMs of the ZnMgO (002) peaks at different annealing temperatures, (c) Sizes of nanoparticles at different annealing temperatures

The images of the ZnMgO nanoparticles can be also observed directly by the SEM measurements. Fig. 2a reveals the typical SEM micrographs of ZnMgO nanocrystals grown by air annealing at 420 ℃. The ZnMgO nanocrystal size gets homogeneous and the surface of the film gets compact, and the nanocrystalline orientation gets linear, but it is worth noticing that ZnMgO thin film annealed at 420 ℃ in vacuum shows raised shape structure and the surface is not smooth. The phenomenon is attributed to the different velocity of recrystallization in different annealing atmosphere. The most smooth and compact crystal surface of ZnMgO thin film is obtained at 420 ℃ by air annealing, which shows that the crystal quality of the ZnMgO thin film annealed is the best at 420 ℃ in air. Fig. 2c shows the EDX spectrum derived from the sample in Fig. 2a. The O, Mg, Zn, Si peaks can be observed, indicating that ZnMgO thin films are fabricated on quartz substrates successfully. In addition, the Au peak was noticed, which was attributed to the fact that the surface of the ZnMgO sample before the examination was coated with a gold thin film in order to enhance the conductivity of the ZnMgO film and facilitate the observation of the surface morphology of the film. In Fig. 2d, the Mg content in the ZnMgO films increases from 2.7 % at 340 ℃ to 3.0 % at 500 ℃ with increasing temperature for air annealing. In addition, for the vacuum annealing, the Mg content appears to increase from 2.9 % at 340 ℃to 3.2 % at 500 ℃. The Mg content of the samples annealed in air is lower than those of the samples annealed in vacuum at the same temperature, suggesting air annealing can reduce the flaw density of the film and promote ZnMgO nanocrystalline growth, which is in accordance with the results of the XRD analysis.

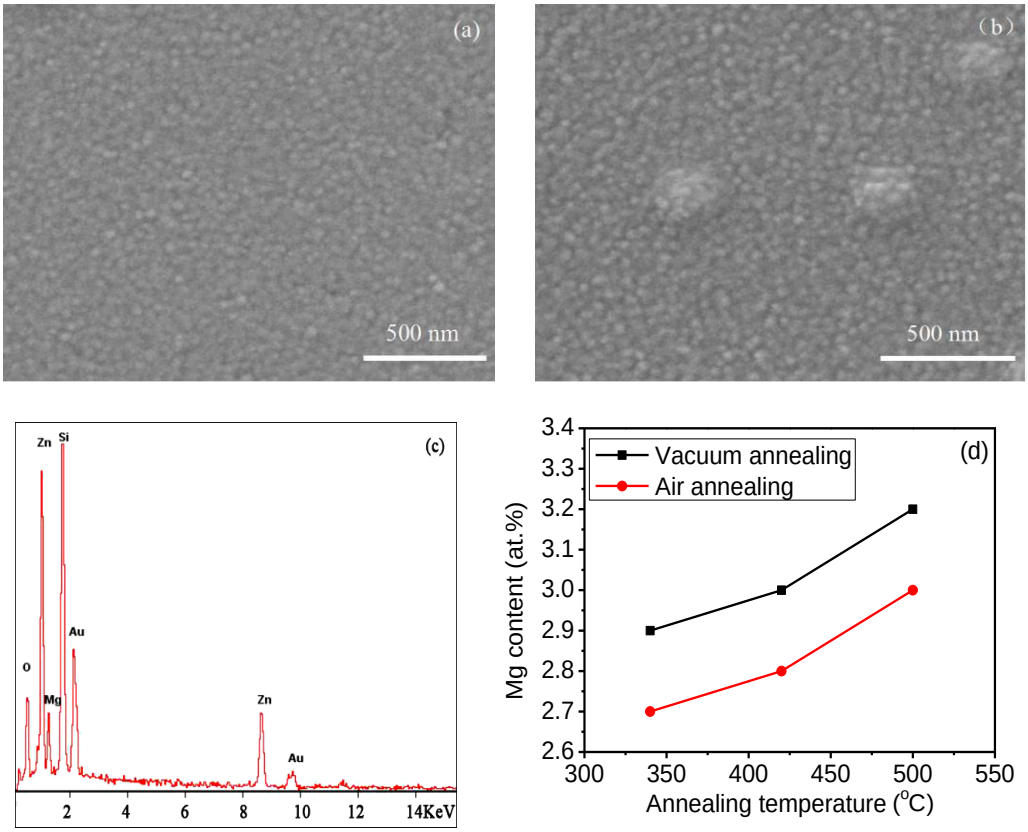

Fig. 2. SEM photographs of ZnMgO annealed at (a) 420 ℃ in air and (b) 420 ℃ in vacuum, (c) EDX spectrum of ZnMgO thin film annealed at 420 ℃ in air, (d) Mg content of the samples at different annealing temperatures

3.2. Optical properties

Fig. 3a, b and c shows the transmittance spectra and the partially enlarged image (the inset) of the ZnMgO films at different annealing temperatures. All the films show the average transmittance more than 80% in visible scope of 340-800 nm, while at the same annealing temperature, the cut-off wavelength always shifts to longer wavelength from 310 nm for the samples annealed in vacuum to 335 nm for the samples annealed in air, denoting the narrowing of the optical band gap with air annealing [24]. The optical band gap (Eg) of the sample can be calculated via Tauc formula [10]:

$$(ahv)^2 = B(hv - Eg) \quad (2)$$

In this formula, hv is the incident photon energy, B is the slope, α is the absorption coefficient, and Eg is the optical band gap. As can be seen from Fig. 3d, the band gaps of the films by air annealing treatment is 3.77 eV, 3.80 eV

and 3.81 eV when the annealing temperature increases from 340 ℃ to 500 ℃. Meanwhile, the band gaps by vacuum annealing treatment are 3.80 eV, 3.81 eV and 3.83 eV from 340 ℃ to 500 ℃. The band gap of the ZnMgO film via air annealing is narrower than that of the vacuum annealing under the same annealing temperature condition, which is consistent with the previous analysis results.

The change of the band gap is deemed to be due to the reduction in Mg content in the ZnMgO films, which is caused by the oxygen in the air ambient. In fact, as depicted in Fig. 2d, Mg content in the $Zn_{1-x}Mg_xO$ films grown at different annealing atmospheres (air and vacuum) by the EDX, the Mg content of air annealing is lower than those of vacuum annealing at the same temperature, indicating a great consistency with the band gap change.

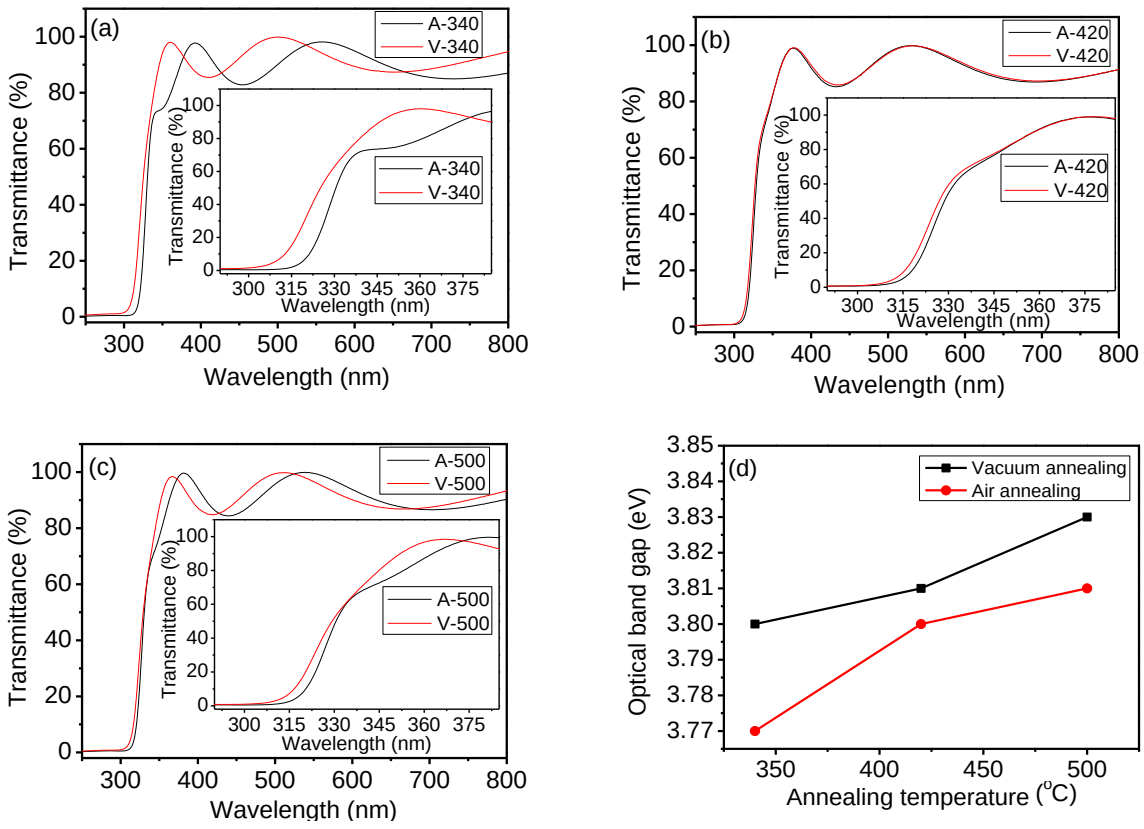

Fig. 3. Transmittance spectra and the partially enlarged image (the inset) of the ZnMgO films annealed at (a) 340 ℃, (b) 420 ℃ and (c) 500 ℃, (d) optical band gaps of the samples at different annealing temperatures

Fig. 4 manifests the PL spectra of ZnMgO thin films annealed at 420 ℃ in air and vacuum. The best four-peak Gaussian fits were performed on the samples, as depicted in Fig. 4a, b. The peak positions via air annealing are located at 585 nm (P1), 632 nm (P2), 693 nm (P3), 777 nm (P4), and the positions of peaks are 588 nm (P1), 630 nm (P2), 678 nm (P3), 740 nm (P4) by vacuum annealing, which may be attributed to the luminescence of ZnMgO nanocrystals (550-850 nm). The intensity of P1-P4 emission peak by air annealing is always higher than that of vacuum annealing, which indicates that the number of ZnMgO nanocrystals is more by air annealing. In addition, as can be seen from Fig. 4c, compared with using the vacuum annealing process, the luminescence peaks of P2-P4 are all red-shifted via adopting air annealing method, and their peaks are at 632 nm, 693 nm, and 777 nm, respectively, demonstrating that the sizes of ZnMgO nanocrystals increase. However, the P1 peak position was blue-shifted a little, and its peak position was 585 nm, indicating that the size of the ZnMgO nanocrystal slightly decreased, which may be originated from the uneven topical growth of the film. In summary, at the unanimous annealing temperature, the emission peak intensity of the film by air annealing is higher than that of the vacuum annealing, and the crystal quality of the film prepared is better through air annealing technique. This is consistent with the analysis results of XRD and SEM.

According to a large number of theoretical references, an important feature of surface dangling bonds existed is the presence of a split surface state band in the band gap, one near the block band gap, and the other surface band positions in the basic band gap are dependent on the surface structure [25-27]. Ivanov et al. [28] showed that there is no surface energy level in the band gap of the bulk material, but it is entirely possible that the surface energy level exists in the corresponding nanoparticles. Therefore, the luminescence band of ZnMgO nanoparticles was obtained between 550-850 nm, indicating that surface

energy levels may exist in the band gap of ZnMgO Nanoparticles. When the air annealing process is used, the oxygen can promote the growth of the ZnMgO nanoparticles, which will lead to a continuous increase in the area-to-volume ratio (specific surface area, S/V) of the nanoparticles, and a significant increase in surface dangling bond density. This will undoubtedly increase the appearance probability of surface energy levels in the energy gap, which the intensity of the emission peak will be increased. The analysis shows that, the emission mechanism of ZnMgO obtained in the range of 550-850 nm by excitation with low photon energy excitation light is different from the reported ZnMgO defect emission.

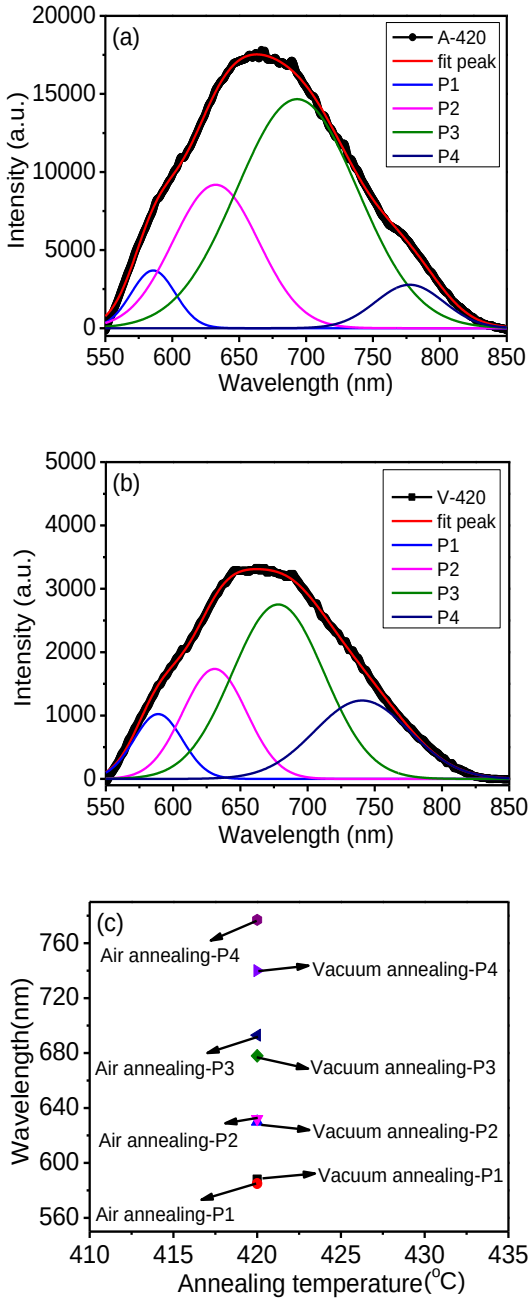

Fig. 4. PL spectrum of ZnMgO annealed at (a) 420 ℃ in air and (b) 420 ℃ in vacuum, (c) Peak position of ZnMgO films annealed at 420 ℃ in air and vacuum

4. Conclusion

ZnMgO thin films were successfully fabricated on the quartz substrate via RF magnetron sputtering and then were annealed in air and vacuum atmosphere, respectively. The effects of annealing atmosphere on structural and optical properties of ZnMgO thin films have been studied methodically. XRD measurements reveal that only hexagonal wurtzite phase exists for all samples. Compared with vacuum annealing, the number of ZnMgO nanocrystals annealed in air is more and the grain size is larger. Meanwhile, SEM image shows that the film prepared by air annealing has better uniformity. From optical transmittance spectra of the samples, the UV absorption edge always shifts to longer wavelength from 310 nm for vacuum atmosphere to 335 nm for air atmosphere, implying the narrowing of the optical band gap with air annealing at the same annealing temperature. The PL spectra show that at the same annealing temperature, the luminescence peak intensity of the ZnMgO nanocrystals annealed in air is larger than that of the vacuum annealing. In addition, the samples annealed with air at 420 ℃ have the most number of nanocrystals and the largest size (19.14 nm). It is expected to prepare high-quality ZnMgO films by optimizing the annealing process, and apply them to the field of optoelectronic devices.

Acknowledgements

This work was financed by the National Science Foundation of China (Grant No. 61704057), Major State Basic Research Development Program of China (Grant No. 2013CB922300), and the Natural Science Foundation of China (Grant No. 61376129).

References

[1] I. S. Kim, B. T. Lee, J. Cryst. Growth **311**, 3618 (2009).
[2] W. Chebil, M. A. Boukadhaba, I. Madhi, A. Fouzri, A. Lusson, C. Vilar, V. Sallet, Physica B **505**, 9 (2017).
[3] M. Tosun, S. Ataoglu, L. Arda, O. Ozturk, E. Asikuzun, D. Akcan, O. Cakiroglu, Mater. Sci. Eng. A **590**, 416 (2014).
[4] A. J. Kulandaisamy, J. R. Reddy, P. Srinivasan, K. J. Babu, G K. Mani, P. Shankar, J. B. B. Rayappan, J. Alloys Compd. **688**, 422 (2016).
[5] A. Singh, A. Vij, D. Kumar, P. K. Khanna, M. Kumar, S. Gautam, K. H. Chae, Semicond. Sci. Technol. **28**, 25004 (2013).
[6] S. Chawla, K. Jayanthi, H. Chander, Phys. Status Solidi **205**, 271 (2008).
[7] Z. K. Heiba, L. Arda, Cryst. Res. Technol. **44**, 845 (2009).
[8] X. Du, Z. Mei, Z. Liu, Y. Guo, T. Zhang, Y. Hou, Z. Zhang, Q. Xue, A. Y. Kuznetsov, Adv. Mater. **21**,

4625 (2009).
[9] J. D. Hwang, S. Y. Wang, S. B. Hwang, J. Alloys Compd. **656**, 618 (2016).
[10] X. Chen, P. Yang, J. Mater. Sci. Mater. Electron. **25**, 5410 14).
[11] T. Maemoto, N. Ichiba, H. Ishii, S. Sasa, M. T. Inoue, J. Phys.: Conf. Ser. **59**, 670 (2007).
[12] S. Sadofev, S. Kalusniak, P. Schafer, S. Sasa, M. Inoue, Appl. Phys. Lett. **102**, 190 (2013).
[13] A. Singh, D. Kumar, P. K. Khanna, A. Kumar, M. Kumar, M. Kumar, Thin Solid Films **519**, 5826 (2011).
[14] H. Liu, R. B. Yang, S. Guo, C. J. Lee, N. L. Yakovlev, J. Alloys Compd. **703**, 225 (2017).
[15] P. Sharma, K. Sreenivas, K. V. Rao, J. Appl. Phys. **93**, 3963 (2003).
[16] H. K. Dong, N. G Cho, K. S. Kim, S. Han, H. G Kim, J. Electroceram. **22**, 82 (2009).
[17] Q. L. Huang, L. Fang, B. D. Guo, H. B. Ruan, F. Wu, C. Y. Kong, J. Optoelectron. Laser **7**, 1021 (2010).
[18] K. Maejima, H. Shibata, H. Tampo, K. Matsubara, S. Niki, Thin Solid Films **518**, 2949 (2010).
[19] X. Q. Wei, R. R. Zhao, Y. J. Wang, L. Y. Liu, B. Q. Cao, Surface Engineering **28**, 678 (2013).
[20] D. P. Xiong, X. G Tang, W. R. Zhao, Q. X. Liu, Y. H. Wang, S. L. Zhou, Vacuum **89**, 254 (2013).
[21] H. B. Cuong, N. M. Le, S. H. Jeong, B. T. Lee, J. Alloys Compd. **709**, 54 (2017).
[22] R. R. Zhao, X. Q. Wei, Y. J. Wang, X. J. Xu, J. Mater. Sci. Mater. Electron. **24**, 4290 (2013).
[23] A. Singh, S. Saini, D. Kumar, P. K. Khanna, M. Kumar, B. Prasad, Phys. Status Solidi **11**, 1488 (2015).
[24] P. Bhattacharya, R. R. Das, R. S. Katiyar, Thin Solid Films **447**, 564 (2004).
[25] M. Schmeits, A. Mazur, J. Pollmann, Phys. Rev. B **27**, 217 (1983).
[26] R. Dorn, H. Luth, M. Buchel, Phys. Rev. B **16**, 4675 (1977).
[27] X. L. Wu, S. J. Xiong, G G Siu, G S. Huang, Y. F. Mei, Z. Y. Zhang, Phys. Rev. Lett. **91**, 157402 (2003).
[28] I. Ivanov, J. Pollmann, Phys. Rev. B **24**, 7275 (1981).

*Corresponding author: jcjiang@ee.ecnu.edu.cn,
fwshi@ee.ecnu.edu.cn